D. G. Truhlar and J. R. Pliego Jr., in *Continuum Solvation Models in Chemical Physics: From Theory to Applications*, edited by B. Mennucci and R. Cammi (Wiley, Chichester, 2008), pp, pp. 338-365.

3.3 Transition State Theory and Chemical Reaction Dynamics in Solution

Donald G. Truhlar and Josefredo R. Pliego Jr.

3.3.1 Introduction

Most chemical and chemical technological processes, including most synthetic and all biochemical reactions, take place in the liquid phase. The solvent often plays a central role in determining the kinetics and outcome of liquid-phase chemical reactions, and the present chapter describes theoretical and computational methods that may be used to understand such effects in terms of continuum solvation models.

How does the solvent influence a chemical reaction rate? There are three ways [1,2]. The first is by affecting the attainment of equilibrium in the phase space (space of coordinates and momenta of all the atoms) or quantum state space of reactants. The second is by affecting the probability that reactants with a given distribution in phase space or quantum state space will reach the dynamical bottleneck of a chemical reaction, which is the variational transition state. The third is by affecting the probability that a system, having reached the dynamical bottleneck, will proceed to products. We will consider these three factors next.

Reactant Equilibrium

In a fixed-temperature gas, molecular collisions populate the various states of the reactants. In the absence of chemical reaction, the populations of these states would come into thermal equilibrium, as governed by Boltzmann statistics (or, in a quantal system, by Fermi–Dirac and Bose–Einstein statistics). However, when reactions occur, the most reactive states (usually the highest-energy ones) may react rapidly. In this case a steady-state distribution is set up in which the rate of population of these states by molecular collisions (and possibly back reaction) is balanced by their depletion by reactions. The resulting nonequilibrium distribution can be quite different from the equilibrium one, especially for unimolecular reactions in low-pressure gases [3,4]. It is often assumed that such nonequilibrium effects are always unimportant in liquids, but this is not necessarily true [5–7]. As a consequence, increasing the strength of solute–solvent couplings may promote a more equilibrated reactant state distribution and thereby change the reaction rate [4]. That is the exceptional case, though, and usually there is no observable nonequilibrium effect [8, 9]. Furthermore, such effects are not usually treated by continuum methods (the subject of this book); hence we will not discuss them in detail in this chapter.

Rate of Attainment of the Transition State

We define a generalized transition state as a hypersurface (usually one just says surface) in phase space separating reactants from products; it is sometimes called a dividing surface. Like any hypersurface, such a dividing surface has one less degree of freedom than the space in which it resides. For any dividing surface that we might define, the reactants must pass through the dividing surface at least once to reach products. One could imagine dividing surfaces that are crossed many times in the course of a typical

reactive event, but these are not very interesting. If one could find a dividing surface such that when reactants reach it, they almost surely go on to products without recrossing the surface, one could calculate a reasonably accurate rate constant by simply calculating the one-way rate of systems passing through the dividing surface. This is transition state theory [10], and the dividing surface is called the transition state. Since a system with an equilibrium distribution in reactant state space will evolve, by Liouville's theorem, into a system with an equilibrium (Boltzmann) distribution in any other part of phase space, including the dividing surface [11, 12], the calculation can be further simplified into a calculation of the *equilibrium* one-way flux through the dividing surface. Notice that an equilibrium flux is independent of the nature of the dynamics that gets the system to the transition state dividing surface; it is even independent of the details of the potential energy surface in the vast expanse of phase space between reactants and the transition state. Calculating reaction rates gets even easier though when one recognizes [13, 14] that the equilibrium rate constant for passing through a dividing surface toward products may be written as

$$k = \frac{k_B T}{h} K^{\ddagger,o} e^{-\Delta G^{\ddagger,o}/RT} \tag{3.15}$$

where k_B is Boltzmann's constant, T is temperature, h is Planck's constant, $K^{\ddagger,o}$ is unity for a unimolecular reaction and the reciprocal of the concentration in the standard state for a bimolecular reaction, $\Delta G^{\ddagger,o}$ is defined by

$$\Delta G^{\ddagger,o} = G^{\ddagger,o} - G^{R,o} \tag{3.16}$$

where $G^{R,o}$ is the standard-state free energy of reactants, and $G^{\ddagger,o}$ is a new quantity that has exactly the same mathematical form as a standard-state free energy but for a system localized in the transition state by having one degree of freedom missing. The degree of freedom that is missing is the coordinate normal to the dividing surface. $G^{\ddagger,o}$ is called the standard-state free energy of the transition state, and $\Delta G^{\ddagger,o}$ is called the standard-state free energy of activation (or sometimes it may be called the standard-state quasithermodynamic free energy of activation). Now the calculation of an equilibrium one-way flux is reduced to the calculation of the difference of two free energies (technically, only $G^{R,o}$ is a free energy; $G^{\ddagger,o}$ is a quasithermodynamic quantity, not a true free energy, because one degree of freedom is missing). Since the transition state is missing one degree of freedom, that degree of freedom must be treated as separable. The missing degree of freedom is usually called the reaction coordinate, and one could say that the separability of the reaction coordinate is the fundamental assumption of transition state theory. (If the reaction coordinate were globally separable there would be no recrossing.) The separability approximation usually breaks down most strongly when tunneling is important, and nonseparability effects can be included by including a multidimensional tunneling contribution as discussed in Section 3.3.2. Even when the separability assumption does not break down for the true variational transition state, i.e., for the true reaction coordinate (any trial transition state, being a dividing surface, defines a trial reaction coordinate as the coordinate normal to it, and vice versa), in practice we are limited to reaction coordinates that depend in a manageable way on only a manageable number of coordinates or that are defined by a simple model, and thus there may be nonseparability (and

hence recrossing) for calculations with practical reaction coordinates. New methods for identifying complex reaction coordinates and reaction coordinates in complex systems are under development [15–17].

The reader will have noticed that at key points in the above discussion we used classical mechanical concepts such as the flux through a dividing surface in phase space. Even the definition of the transition state (as a phase-space dividing surface) is classical. In fact there is no unique way to extend the definition of the transition state to quantum mechanics. However, if we write the free energies in terms of statistical mechanical quantities such as partition functions, there are well-known ways to replace classical mechanical partition functions by quantal ones. We will return to this issue and other practical issues involved in evaluating and improving Equation (3.15) in Section 3.3.2. However first we need to introduce another concept that will be important in computing free energies in liquid-phase solution, namely the concept of potential of mean force (PMF). The PMF is a statistical mechanical quantity that corresponds to the free energy for a system in which one or more coordinate is 'nailed down,' that is constrained to a constant value. For example a two-dimensional PMF corresponds to fixing two coordinates; they could be the x and y Cartesian coordinates of one of the atoms or – more likely in applications – they might be some functions of the internal coordinates such as the distance from atom A to atom B and the distance from atom B to atom C. (Note that distances are nonlinear functions of the atomic Cartesian coordinates; we call them curvilinear coordinates, whereas linear functions of atomic Cartesians are called rectilinear coordinates.)

In general, if H is the Hamiltonian of the system, i.e., its total energy, the free energy G is defined by

$$e^{-G/RT} = \langle e^{-H/RT} \rangle \tag{3.17}$$

where $< \ldots >$ denotes a Boltzmann average over all phase space at temperature T. We label the set of constrained coordinates of a PMF calculation as $\mathbf{R}$, the set of other coordinates as $\mathbf{r}$, and the set of all conjugate momenta as $\mathbf{p}$. Then Equation (3.17) becomes

$$e^{-G/RT} = \langle e^{-H/RT} \rangle_{\mathbf{R},\mathbf{r},\mathbf{p}} \tag{3.18}$$

Alternatively we can carry this out in two steps

$$e^{-W(\mathbf{R})/RT} = \langle e^{-H/RT} \rangle_{\mathbf{r},\mathbf{p}} \tag{3.19}$$

$$e^{-G/RT} = \langle e^{-W(\mathbf{R})/RT} \rangle_{\mathbf{R}} \tag{3.20}$$

This defines $W(\mathbf{R})$ as the PMF of coordinates $\mathbf{R}$. For applications we need to specify whether a constant of integration is added to G or W to set their zero of energy [18].

The standard-state solvation free energy ΔG_S° of a solute corresponds to a statistical average over its coordinates, which may be called $\mathbf{R}$, and the coordinates of the solvent, which may be called $\mathbf{r}$. By analogy to the PMF we may define a constrained standard-state free energy of solvation as

$$\Delta G_S^\circ(\mathbf{R}) = W(\mathbf{R}) - V(\mathbf{R}) \tag{3.21}$$

where $W(\mathbf{R})$ is the liquid-phase PMF of the solute molecule, and $V(\mathbf{R})$ is the gas-phase potential energy of that molecule. Again we need to be careful about additive constants that account for standard states and zeroes of energy. According to the Born–Oppenheimer approximation [19], $V(\mathbf{R})$ is given by the electronic energy of the molecule with fixed nuclear coordinates $\mathbf{R}$. (The electronic energy is defined [19] to include the internuclear Coulomb repulsion.)

Equation (3.21) shows that the potential of the mean force is an effective potential energy surface created by the solute–solvent interaction. The PMF may be calculated by an explicit treatment of the entire solute–solvent system by molecular dynamics or Monte Carlo methods, or it may be calculated by an implicit treatment of the solvent, such as by a continuum model, which is the subject of this book. A third possibility (discussed at length in Section 3.3.3) is that some solvent molecules are explicit or discrete and others are implicit and represented as a continuous medium. Such a mixed discrete–continuum model may be considered as a special case of a continuum model in which the solute and explicit solvent molecules form a supermolecule or cluster that is embedded in a continuum. In this contribution we will emphasize continuum models (including cluster–continuum models).

Recrossing

Transition state theory, as explained above, assumes an equilibrium distribution in reactant state space and no recrossing of the transition state. In a classical mechanical world, we could always find a transition state that is not recrossed, but – except very close to threshold [20] – the resulting dividing surface would typically be so convoluted that it would be impossible to use. A better strategy [21] is to find the best (but not perfect) dividing surface from among a sequence of practical dividing surfaces. Then one corrects the approximate transition state theory rate expression for recrossing by multiplying by a transmission coefficient. The best transition state is the one that minimizes the amount of recrossing, which corresponds to minimizing the one-way flux [22]. This best transition state is called the variational transition state, and its use to calculate reaction rates is called variational transition state theory [21–25]. Often when we say 'transition state,' it is shorthand for 'variational transition state' or 'best transition state' or 'dynamical bottleneck' although the phrase may also be used to refer to trial transition states.

A new issue arises when one makes a solute–solvent separation. If the solvent enters the theory only in that $V(\mathbf{R})$ is replaced by $W(\mathbf{R})$, the treatment is called equilibrium solvation. In such a treatment only the coordinates in the set $\mathbf{R}$ can enter into the definition of the transition state. This limits the quality of the dynamical bottleneck that one can define; depending on the system, this limitation may cause small quantitative errors or larger more qualitative ones, even possibly missing the most essential part of a reaction coordinate (in a solvent-driven reaction). Going beyond the equilibrium solvation approximation is called nonequilibrium solvation or solvent friction [4, 26–28]. This is discussed further in Section 3.3.2.

Application Areas

Continuum solvation models have been applied to many chemical processes in the liquid phase. Determining absolute free energies of activation is important because it allows one to predict the time scale on which a chemical process can take place. In addition,

the absolute barrier height is critical for determining mechanisms of chemical processes whose reaction pathway is not well known from experiment.

There are four important problem areas where the study of chemical reactions in solution can be very useful. The first class of problems involves calculating the absolute free energy of activation or rate constant. Our ability to predict absolute reaction rates is critical in order to determine if a reaction can take place or not. A high free energy of activation indicates that a reaction is slow or does not occur or that the true reaction pathway was not found. In other cases, there is a clear experimental observation of the reaction, but the calculated barrier of the supposed mechanism is very high. In this case, if we assume that a sufficiently reliable level of electronic structure theory was used to calculate the barrier, it means that we do not know the real mechanism and a more detailed investigation should be done. This leads us to the second problem: elucidating the reaction mechanism. Although for some chemical processes the reaction mechanism is known, for many reactions the true mechanism is not known at all. In other cases, there are doubts about the real mechanism. These problems are discussed further in Section 3.3.4. The third problem is the competition between parallel pathways. The relative rate constants determine the product ratio. Thus, our ability to calculate relative rate constants allows us to predict which product is generated in a chemical reaction. An interesting application is to predict the products of a reaction of synthetic interest, which may result from a competition such as that between S_N2 and E2 process. This is discussed in Section 3.3.5. Another example of the need to calculate relative reaction rates is kinetic isotope effects, i.e., the relative rates of reaction of different isotopomers or isotopologs. Kinetic isotope effects are often used by experimentalists to elucidate reaction mechanisms and to gain an understanding of the nature of the transition state (i.e., of the dynamical bottleneck). They are discussed in Section 3.3.4.

The fourth aspect is related to development of more efficient reaction media or catalysts. The dream of a chemist is to be able to induce a chemical transformation to take place quickly, efficiently, selectively, and with good specificity. Computational studies of reactions in solution allow us to understand the factors that influence reactivity and enable us to design new catalysts or solvent media with better properties. Because continuum models are fast, easy to use, and often reliable, they may be chosen for theoretical studies aimed at the development of catalysts or chemical processes.

Examples of applications will be presented later in this contribution. However, first we will discuss transition state theory for liquid-phase reactions and parametrization of continuum models for reactive problems, because these theoretical constructs are required for applications to chemical reactions in the liquid phase.

3.3.2 Transition State Theory

The most useful theoretical framework for studying chemical reactions in solution is transition state theory. Building on the material presented in the introduction, we will begin by presenting a general theory called the equilibrium solvation path (ESP) theory of reactions in a liquid. We then present an approximation to ESP theory called separable equilibrium solvation (SES). Finally we present a more complete theory, still based on an implicit treatment of solvent, called nonequilibrium solvation (NES). All three

theories assume reactant equilibrium, as discussed in the introduction. (Simple methods for including nonequilibrium reactant effects are reviewed elsewhere [29].) In discussing the ESP and the SES theories, **R** is always the set of atomic coordinates of an N-atom solute, although (as mentioned above) one may, if desired, include one or a few solvent molecules as part of the 'solute' (the so called 'supermolecule' approach).

Equilibrium Solvation Path (ESP)

In ESP theory [30–32] we treat the system by the same methods that we would use in the gas phase except that in the nontunneling part of the calculation we replace $V(\mathbf{R})$ by $W(\mathbf{R})$, and in the tunneling part we approximate $V(\mathbf{R})$ by $W(\mathbf{R})$ or a function of $W(\mathbf{R})$. Next we review what that entails. In particular we will review the application of variational transition state theory [21–25] with optimized multidimensional tunneling [33, 34] to liquid-phase reactions for the case [31,32] in which $W(\mathbf{R})$ is calculated from $V(\mathbf{R})$ by

$$W(\mathbf{R}) = V(\mathbf{R}) + \Delta G_S^\circ(\mathbf{R}) \tag{3.22}$$

and the constrained standard-state free energy of solvation is obtained by a continuum solvation model. Notice that we follow the usual practice of not indicating explicitly that $W(\mathbf{R})$ depends on the standard state, although it does.

The conventional definition of the transition state is a hyperplane passing through the saddle point of $V(\mathbf{R})$ and orthogonal to the imaginary-frequency normal mode [10,13,14, 35,36]. This definition can also be applied using a saddle point of $W(\mathbf{R})$ and normal mode analysis of $W(\mathbf{R})$ instead of those for $V(\mathbf{R})$. Call this saddle point geometry $\mathbf{R}^\ddagger$. Note (from the definition of $W(\mathbf{R})$ given above) that a saddle point of $W(\mathbf{R})$ corresponds to an average over an ensemble of solvent configurations at solute geometry $\mathbf{R}^\ddagger$. This does not correspond to a saddle point of the potential energy of the entire (solute+solvent) system. For that reason it is a misnomer to call the theory based on $W(\mathbf{R})$ conventional transition state theory. In fact the conventional idea of calculating the rate constant using a dividing surface that passes through a saddle point of the entire system is not suitable for reactions in liquids because there are an uncountable number of saddle points, most of which differ only in the conformation of some far-away solvent molecules (by conformation here we mean not just intramolecular conformation but also hydrogen-bonding and noncovalent-packing conformations of interacting solvent molecules). Thus, in the early days of transition state theory, the theory was generalized [37,38] to liquid-phase reactions by stating it in thermodynamic or statistical thermodynamic language. This obviated the need to define clearly the transition state for liquid reactions, and this task was only taken up more recently by using the concept of the PMF.

In the next step, one finds the minimum (free) energy path (MEP) starting at $\mathbf{R}^\ddagger$ and follows it toward both reactants and products. The progress variable s that measures the signed distance along the path from the saddle point is called the reaction coordinate, although that name is also used (see above) for the missing degree of freedom in the transition state, and the two coordinates are not always the same (a possible point of confusion, but both usages of 'reaction coordinate' are so well established that there can be no turning back). This path is defined as the path of steepest descents, which in general depends on the coordinate system in which it is computed [39]. In this chapter,

when we refer to the MEP we always mean the one computed in mass-scaled or mass-weighted rectilinear coordinates that diagonalize the classical mechanical kinetic energy; such coordinate systems are called isoinertial, and the MEP is the same in any such coordinate system [40]. The reasons for choosing an isoinertial coordinate system are that it promotes the local separability of the reaction coordinate, and it allows intuition about the motion of N atoms in three dimensions as if it were the motion of a single mass point in $3N$ dimensions [39–42]. The MEP is sometimes called the intrinsic reaction path or intrinsic reaction coordinate [43].

One next defines a sequence of dividing surfaces, which are trial transition states (these are sometimes called generalized transition states to denote that they are not conventional transition states at saddle points, but we will drop this semantic distinction here). Usually one uses a one-parameter sequence of dividing surfaces, either hyperplanes in a rectilinear coordinate system [21,40,44,45] or curved dividing surfaces defined in valence internal coordinates [46,47]. The parameter is the value of s at which the transition state, locally orthogonal to the MEP, intersects the MEP, and one optimizes this value to find the variational transition state location, which is called s_*. The deviation of s_* from the location along the MEP where potential energy is a maximum is called a variational effect. More generally one can variationally optimize not only the value of the reaction coordinate but also the orientation of the dividing surface; this approach can even be applied without computing the MEP [48,49]. One can also use dynamically optimized reaction paths that pass through a sequence of variationally optimized multi-parameter dividing surfaces [50].

For each dividing surface one calculates the free energy of the transition state by standard statistical mechanical procedures in terms of partition functions by treating the transition state as a molecule with one degree of freedom missing [35,36]. The standard-state free energy of activation is then obtained from Equation (3.16).

An alternative procedure for calculating $G^{\ddagger,o}$ would be to calculate a one-dimensional PMF, in particular $W(s)$ or $W(z)$, where z is the distance along an arbitrary reaction path, and note that

$$G^{\ddagger,o} = W(z_*) + W_{curv}(z_*) \tag{3.23}$$

where $W_{curv}(z)$ is a term, often but not always negligible, that vanishes when the missing degree of freedom is rectilinear [18]. We shall not pursue this here.

Since we replaced the classical partition functions in $G^{R,o}$ and $G^{\ddagger,o}$ by quantum mechanical ones, we have included quantum effects on all degrees of freedom of the reactants and all but the missing degree of freedom at the transition state. One then includes quantum effects on the remaining degree of freedom by a transmission coefficient κ, thereby replacing Equation (3.15) by

$$k = \kappa \frac{k_B T}{h} K^{\ddagger,o} e^{-\Delta G^{\ddagger,o}/RT} \tag{3.24}$$

Note that both κ and $\Delta G^{\ddagger,o}$ depend on temperature. The transmission coefficient is sometimes called the tunneling transmission coefficient because tunneling is the main quantum effect on the reaction coordinate.

The derivation of transition state theory as the flux through a dividing surface assumes that the system can be in the transition state only when it has positive classical mechanical kinetic energy there [14]. Tunneling is the phenomenon by which a particle passes through a barrier which it cannot pass through with positive classical mechanical kinetic energy. (Other definitions of tunneling are possible and sometimes preferable, but will not be used here.) Since reaction by tunneling may occur where the Boltzmann factor is much larger than that for overbarrier reaction, its contribution to the reaction rate may be large even when the tunneling probability is small. An analogous nonclassical effect is called nonclassical reflection. Tunneling and nonclassical reflection may both be understood in terms of a particle of energy E impinging on a one-dimensional barrier $V(z)$ with barrier height $V^{\ddagger}$. Classically the particle has zero transmission probability for $E < V^{\ddagger}$ (this is classical reflection) and unit transmission probability for $E > V^{\ddagger}$ (this is classical transmission). The fact that a quantum mechanical particle has nonzero probability of transmission for $E < V^{\ddagger}$ is called tunneling (or nonclassical transmission), and the fact that it has nonunit probability of transmission for $E > V^{\ddagger}$ is called nonclassical reflection (or diffraction by the barrier). The two phenomena have similar magnitudes; for example, for a purely parabolic barrier, the tunneling probability at energy $E = V^{\ddagger} - \Delta$ is the same as the nonclassical reflection probability at $E = V^{\ddagger} + \Delta$; however, tunneling usually has a much greater effect on reaction rates because it occurs at energies that have an exponentially larger Boltzmann factor [51].

One-dimensional treatments of tunneling are not reliable [52]. For gas-phase reactions, accurate multidimensional tunneling approximations have been developed [33,34,53–55] and are well validated against accurate quantum mechanical calculations [56,57]. These tunneling approximations are nonseparable, and using them to calculate κ overcomes (at least partially) the separability assumption of transition state theory. In fact when tunneling dominates the reaction rate and is modeled by multidimensional tunneling approximations, the calculation is better viewed as a semiclassical multidimensional dynamics calculation than as transition state theory. To extend these methods to liquid-phase reactions modeled by continuum solvation methods one needs to know the effective potential for tunneling. The PMF is already averaged over a canonical ensemble of solvent configurations and, like any free energy quantity, it includes entropy as well as potential energy; thus it is not *a priori* clear that it can be used to provide the effective barrier for tunneling. In principle one would calculate the tunneling from the potential energy and ensemble average [26,27,31] the tunneling probabilities. A more practical (but approximate) procedure is to calculate the tunneling from the ensemble-averaged potential energy. It can be shown [31] that the canonically averaged mean potential energy is given (within an additive constant, which is all that is required) by

$$U = V(\mathbf{R}) + \Delta G_S^{\circ}(\mathbf{R}) - T\frac{\partial G(\mathbf{R})}{\partial T} \tag{3.25}$$

Neglect of the last term yields Equation (3.22), which is called (in this context) the zero-order canonical mean-shape (CMS-0) approximation [31].

Separable Equilibrium Solvation (SES)

In the SES approximation [32] we make some simplifications in the ESP formalism. First, the saddle point is optimized using $V(\mathbf{R})$ rather $W(\mathbf{R})$, and the MEP is also traced using

$V(\mathbf{R})$. In calculating transition state partition functions along s and in calculating reactant partition functions, $W(\mathbf{R})$ is used instead of $V(\mathbf{R})$ at the minimum energy structure of each transition state or reactant, but vibrational frequencies are calculated using $V(\mathbf{R})$. In tunneling calculations, as in ESP theory, $U(\mathbf{R})$ is used instead of $V(\mathbf{R})$. The CMS-0 approximation is usually made in computing $U(\mathbf{R})$.

SES theory can be used to illustrate a classic example of a solvent effect on a chemical reaction, namely the solvent effect on bimolecular nucleophilic substitution (S_N2) reactions [58]. Figure 3.8 shows how an approximate potential of mean force changes with the solvent. We can see that in the gas phase, the barrier is very low. In aqueous solution, the anion is very well solvated, and the formation of the transition state leads to considerable charge delocalization, decreasing the favorable solvation effect. As a consequence, a very high effective barrier is generated. In dipolar aprotic solvents, such as dimethyl sulfoxide, because the ionic species are less solvated than in water, the solvent effect decreases, producing the well-known [59] rate acceleration of ionic S_N2 reactions on going from aqueous to dipolar aprotic solvents.

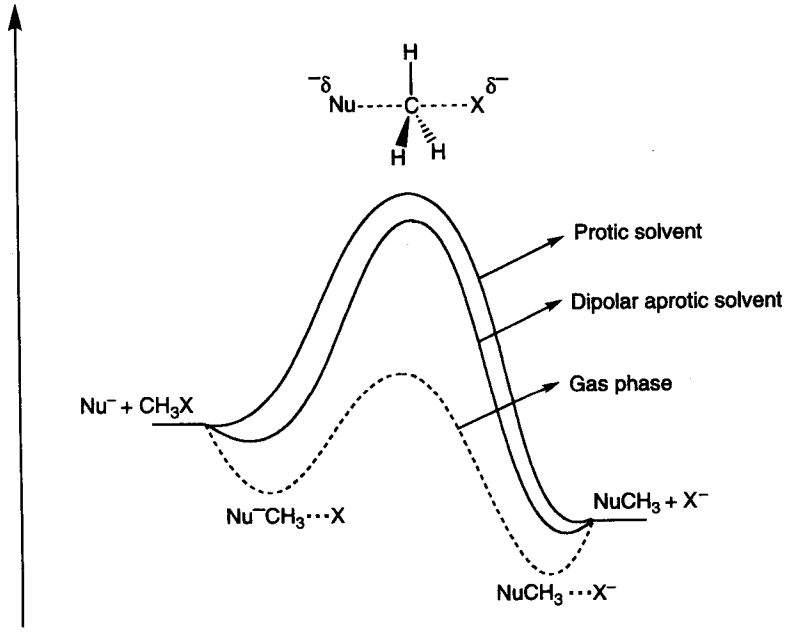

Figure 3.8 *Potential of mean force profile for a typical S_N2 reaction in different media.*

Nonequilibrium Solvation (NES)

In the above treatments only the solute coordinates **R** appear explicitly and therefore the definition of the transition state does not depend on solvent coordinates. The NES approximation [60,61] provides a way to include solvent in the reaction coordinate while retaining a continuum description of the solvent by adding a coupling Hamiltonian for a collective solvent coordinate [60–70] (or more than one) to the Hamiltonian for the

R degrees of freedom. (Sometimes the collective solvent coordinate is assumed to be the reaction coordinate itself [70] rather than, as here, finding a reaction coordinate in the space obtained by augmenting the solute coordinates by the collective solvent coordinate.) As in ESP theory, in NES theory the equilibrium solvent effects are included by replacing $V(\mathbf{R})$ by $W(\mathbf{R})$ in nontunneling parts of the calculation and by $U(\mathbf{R})$ in tunneling algorithms.

Consider the case of a single collective solvent coordinate y. This coordinate is linearly coupled to the solute at the transition state by generalized Langevin theory [71–75]. (It is not necessary to couple the solvent to the solute for the calculation of reactant properties because we retain the equilibrium-reactant approximation.) The form of the coupling is [60,61]

$$H_{\text{coupling}} = \frac{p_y^2}{2\mu} + \frac{1}{2}F\left[y - \mathbf{C}^{\mathrm{T}}\left(\mathbf{R} - \mathbf{R}^{\ddagger}\right)\right]^2 \tag{3.26}$$

where p_y is the momentum conjugate to y, μ is the reduced mass to which all coordinates are scaled (this will cancel out and have no effect on the dynamical results), F is a collective solvent force constant, **C** is a solute–solvent coupling vector with components C_i, and T denotes a transpose. The parameter F may be related to the solvent relaxation time, and the coupling constants may be related to some measure of the strength of the solute–solvent coupling, such as viscosity or diffusion coefficient from experiment or the force autocorrelation function from explicit-solvent molecular dynamics simulations [60]. Solvent relaxation times can be modeled either by explicit-solvent simulations [76–79] or by continuum models [62,65,74,79–86].

The SES, ESP, and NES methods are particularly well suited for use with continuum solvation models, but NES is not the only way to include nonequilibrium solvation. A method that has been very useful for enzyme kinetics with explicit solvent representations is ensemble-averaged variational transition state theory [26,27,87] (EA–VTST). In this method one divides the system into a primary subsystem and a secondary one. For an ensemble of configurations of the secondary subsystem, one calculates the MEP of the primary subsystem. Thus the reaction coordinate determined by the MEP depends on the coordinates of the secondary subsystem, and in this way the secondary subsystem participates in the reaction coordinate.

Other methods of including nonequilibrium solvation are reviewed elsewhere [86], and the reader is also referred to selected relevant and more recent original papers [66,88–100]. Particularly relevant to the present volume are methods that introduce extra degrees of freedom by using the solvent reaction field not only at the current value of **R** but also at nearby values [65,66]. Many of the approaches introduce finite-time effects and additional degrees of solvent freedom by introducing different time scales for electronic and atomic polarization [88–97,99,100].

In the absence of discrete solvent molecules or a collective solvent coordinate, continuum solvation models do not allow the solvent to enter into the reaction coordinate, and in many cases that misses the primary role of the solvent. The solvent may enter the reaction coordinate only quantitatively, for example by having a slightly different strength of hydrogen bonding to the solute at the transition state than at the reactant, or it may enter qualitatively, for example by entering or leaving the first solvation shell, by

donating or accepting a proton (later being regenerated by another proton transfer so it remains a catalyst, not a reagent), and so forth. Some examples of solvent participation in the reaction coordinate that cannot be mimicked without explicit solvent molecules occur in the formamidine rearrangement [101, 102] and in the Beckmann rearrangement [103] of oximes.

3.3.3 Parameterization of Continuum Models for Dynamics

Continuum solvation models consider the solvent as a homogeneous, isotropic, linear dielectric medium [104]. The solute is considered to occupy a cavity in this medium. The ability of a bulk dielectric medium to be polarized and hence to exert an electric field back on the solute (this field is called the reaction field) is determined by the dielectric constant. The dielectric constant depends on the frequency of the applied field, and for equilibrium solvation we use the static dielectric constant that corresponds to a slowly changing field. In order to obtain accurate results, the solute charge distribution should be optimized in the presence of the field (the reaction field) exerted back on the solute by the dielectric medium. This is usually done by a quantum mechanical molecular orbital calculation called a self-consistent reaction field (SCRF) calculation, which is iterative since the reaction field depends on the distortion of the solute wave function and vice versa. While the assumption of linear homogeneous response is adequate for the solvent molecules at distant positions, it is a poor representation for the solute–solvent interaction in the first solvation shell. In this case, the solute *sees* the atomic-scale charge distribution of the solvent molecules and polarizes nonlinearly and system specifically on an atomic scale (see Figure 3.9). More generally, one could say that the breakdown of the linear response approximation is connected with the fact that the liquid medium is structured [105].

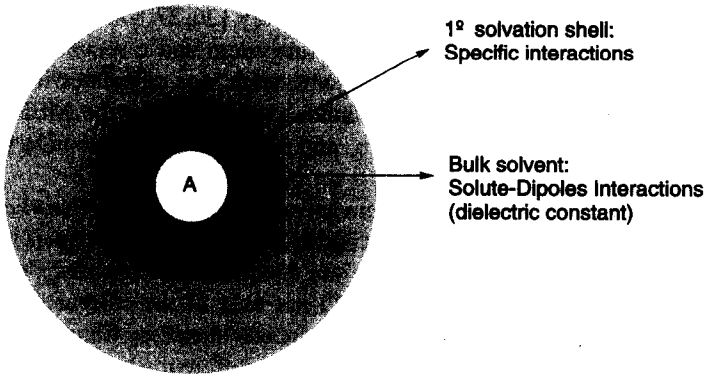

Figure 3.9 *Interaction of the solute with the first solvation shell and with the bulk solvent.*

The solvation free energy calculated by considering only the bulk electrostatics is somewhat arbitrary because the boundary between the dielectric medium and the solute is not well defined, and in fact the treatment of the solvent as a homogeneous, isotropic, linear medium right up to a definite boundary is not valid. To obtain an accurate solvation

free energy, we can use various empirical procedures. These procedures may involve empirical adjustments of the location of the solute–solvent boundary, and/or they may involve introducing additional terms that depend on the solute–solvent boundary. An important point about the components of a solvation energy calculation is that they have no real meaning as thermodynamic variables; only the sum of all the components of the free energy of solvation is meaningful. This is well illustrated by a systematic comparison of three solvation models that was recently reported; the bulk electrostatic terms differed greatly, but after adding each model's nonbulk electrostatic terms, the resultant free energies of solvation were in better agreement [106].

Adding additional terms to account for system-specific first-solvation shell interactions works well for neutral solutes, especially if the additional terms are well parameterized. This strategy has been used in the SMx models [69,107] ($x = 1$–6), where the parameters are atomic surface tensions, where a surface tension is a free energy per unit area. In later versions of these models the area in question here is the solvent-exposed surface area of a given atom of the solute, and the atomic surface tensions depend on the local bonding geometry of the atom in question [107–115]. These dependences are built into parameterized, continuous functions of geometry in such a way that they are well defined at transition states, and furthermore the user is not required to assign molecular mechanics types to the atoms. One expects that the scheme works at least in part because the partial atomic charge, polarizability, and atomic size of each atom of the solute are functions of its local bonding geometry. This procedure is less satisfactory for charged solutes where these properties are not the same functions of geometry as for neutral solutes. Allowing the atomic surface tensions to depend explicitly on local charge would solve this problem, but would complicate the algorithm, requiring the first-solvation-shell effects to be self-consistently adjusted during the SCRF iterations. An alternative approach is to treat some or all of the solvent molecules in the first solvation shell, especially those near highly concentrated regions of partial charge in the solute, as parts of an extended solute, called the supermolecule. Pliego and Riveros [116] call this the cluster–continuum model, whereas other researchers call it a mixed discrete–continuum approach. Pliego and Riveros [116] have provided a protocol for how many explicit solvent molecules should be included, whereas Kelly *et al.* [117] have suggested that one solvent molecule is usually sufficient.

Pratt and co-workers have proposed a quasichemical theory [118–122] in which the solvent is partitioned into inner-shell and outer-shell domains with the outer shell treated by a continuum electrostatic method. The cluster–continuum model, mixed discrete–continuum models, and the quasichemical theory are essentially three different names for the same approach to the problem [123]. The quasichemical theory, the cluster–continuum model, other mixed discrete–continuum approaches, and the use of geometry-dependent atomic surface tensions provide different ways to account for the fact that the solvent does not retain its bulk properties right up to the solute–solvent boundary. Experience has shown that deviations from bulk behavior are mainly localized in the first solvation shell. Although these first-solvation-shell effects are sometimes classified into cavitation energy, dispersion, hydrophobic effects, hydrogen bonding, repulsion, and so forth, they clearly must also include the fact that the local dielectric constant (to the extent that such a quantity may even be defined) of the solvent is different near the solute than in the bulk (or near a different kind of solute or near a different part of the same solute). Furthermore

since the atomic radii and the atomic surface tensions are usually determined empirically, they must also make up for systematic errors in the solute charge distributions and for the fact that actually the solute–solvent boundary is gradual and fluctuating, not sharp and fixed.

Returning to the calculation of the bulk electrostatic contribution to the free energy of solvation, first one needs to define the size and shape of the cavity. Although some older continuum models used spherical or other idealized shapes (e.g. ellipsoids), most modern continuum models use realistic cavity shapes based on superposition of atom-centered spheres. There is, however, no consensus on the radii to be assigned to these atomic spheres. For the purpose of parameterizing the atomic radii, it is especially useful to consider the solvation of ionic species because the solvation free energy of these species has a high absolute value and is very sensitive to the atomic radii. Solvation data for organic ions are widely available for water [124–126], dimethyl sulfoxide (DMSO) solutions [126], and assorted other solvents [127], and these have been used to parameterize continuum models in many solvents [114, 115, 117, 127–129]. Comparing the performance of the parametrizations of continuum models for pK_a calculations in water and DMSO illustrates the reliability that can be achieved. It was shown that polarized continuum models can predict pK_a values in DMSO solution [130, 131] with an error of only two units. These results indicate that these models can be used for semiquantitative modeling of ionic reactions in dipolar aprotic solvents. On the other hand, in water or protic solvents, the performance of continuum models is worse because of strong hydrogen bonds between the ionic species and the water molecules or because of the unique cooperative hydrogen bonding structure of liquid water. No set of atomic radii is capable of producing very accurate solvation free energy values for all situations. Nevertheless, by including some explicit water molecules in the first solvation shell in order to account for critical solute–solvent hydrogen bonds and for strong electrostatic interactions, one can obtain more accurate results. In this approach, the solute–water cluster becomes the new solute (Figure 3.10). In the calculation of pK_a values in water solution,

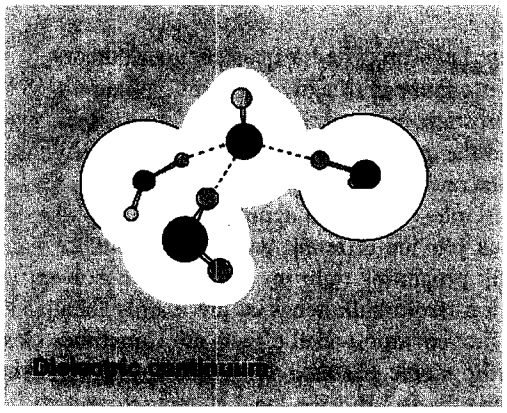

Figure 3.10 *Inclusion of the first-solvation-shell interaction for the solvation of the hydroxide ion in water solution.*

it was shown that the cluster–continuum method works much better than pure continuum models [132].

One special difficulty of applying parameterized models to chemical reactions deserves a special mention, namely that transition states often have charge distributions quite different from those against which solvation models are parameterized. For example, the partial atomic charge on Cl in the $(Cl\ldots CH_3\ldots Cl)^{-1}$ S_N2 transition state is about -0.7, midway between the values (-1.0 and about -0.4, respectively) found in Cl^- monatomic anion and typical alky chlorides. Thus the atomic radii and atomic surface tensions optimized against equilibrium free energies needs to be re-validated for transition structures.

In principle, we can distinguish two possible kinds of breakdown of continuum solvation models as they are usually applied to dynamics problems. One is breakdown of the linear response approximation, and the other is breakdown of equilibration solvation. Although these are different, they sometimes occur in tandem. It is worthwhile to sort these issues out in a little more detail. If one considers very small deviations from equilibrium, the solvent response is formally linear since one can always make the deviation from equilibrium so small that the first term dominates the expansion in powers of the deviation. However in practice, the computations may require more than this. For example to calculate an equilibrium free energy of solvation one may require linear response over the entire range of solute–solvent coupling from zero coupling (solute in gas phase) to full coupling (solute fully inserted in solvent). Even for this large range of coupling, it may be reasonable to assume linear response of the bulk electrostatic effect, but the response of the first solvation shell may show appreciable nonlinearity. The approaches mentioned above can account for this in various ways, e.g. by using a nonbulk dielectric constant in the first solvation shell, by treating all or part of the first solvation shell explicitly, or by including empirical atomic surface tensions on the solute. These same issues occur for dynamics, and they are compounded by the fact that the deviation from equilibrium is finite, so the formal justification for linear response is no longer applicable. In fact the assumption of linear response may even be qualitatively wrong for a nonequilibrium situation, such as the energy relaxation of a highly excited mode produced by photoexcitation or reaction [105]. A quantitative assessment of the effect of nonlinear response on calculated thermal reaction rates is not available, but the assumption that it is small or can be modeled by the methods mentioned above has worked well.

3.3.4 Absolute Free Energy Barriers, Reaction Mechanisms, and Kinetic Isotope Effects

The standard-state free energy of activation for a liquid-phase reaction is

$$\Delta G^{\ddagger,\circ} = \Delta G^{\ddagger,\circ}(g) + \Delta\Delta G_S^{\ddagger,\circ} \tag{3.27}$$

where the first term on the right-hand side is the gas-phase (g) value, and the second term is the solvation contribution given by

$$\Delta\Delta G_S^{\ddagger,\circ} = \Delta G_S^{\ddagger,\circ} - \Delta G_S^{R,\circ} \tag{3.28}$$

where the superscript R denotes the value for reactants. As discussed above, the solvation free energy includes a bulk electrostatic contribution and nonbulk electrostatic terms. The bulk electrostatic term can be calculated by the dielectric continuum model and is the largest contribution for ionic reactions. The other terms make a smaller contribution for ions, but for reactions involving neutral species, where the bulk electrostatic term is less important, nonbulk electrostatic solvation can be significant or even dominant. These terms can be calculated by empirical models.

In addition to SM*x* and the cluster–continuum model, other continuum models have also been used to study reactions in liquids, including the polarized continuum model [133–135] (PCM), the conductor-like screening model (COSMO [136] and COSMO–RS [137, 138]), the generalized COSMO [139] (GCOSMO) model, conductor-like PCM [140] (CPCM), and isodensity PCM [141] (IPCM).

Ionic reactions are especially interesting because they can have a large solvent effect. In the past 10 years, the important class of ionic S_N2 reactions have been studied through *ab initio* calculations coupled with continuum solvation models in different media [32, 142–150]. In the case of dipolar aprotic solvents, the performance of the continuum models is very good. Tondo and Pliego [147] have investigated the S_N2 reaction of CH_3COO^- with ethyl halides: $CH_3COO^- + CH_3CH_2X \rightarrow CH_3COOCH_2CH + X^-$, (X = Cl, Br, I). They have used MP4/CEP-31+G(d)//MP2/CEP-31+G(d) electronic structure calculations and the Pliego–Riveros parametrization of the PCM model for DMSO solvent [128]. The standard-state free energies of activation were calculated to be 24.9, 20.0, and 18.5 kcal mol^{-1}, while the experimental values are 22.3, 20.0, and 16.6 kcal mol^{-1}, respectively. Thus, the theoretical calculations were able to predict the correct reactivity order. Another S_N2 reaction that was studied using this same PCM parametrization for DMSO solvent is the interaction of the cyanide ion with ethyl chloride [149]: $CN^- + CH_3CH_2Cl \rightarrow CH_3CH_2CN + Cl^-$. The solution phase $\Delta G^{\ddagger,o}$ calculated at the CCSD(T)/6-311+G(2df,2p)//B3LYP/6-31G(d) electronic structure level is 24.1 kcal mol^{-1} and it is in excellent agreement with the experimental [151] value of 22.6 kcal mol^{-1}. On average, these theoretical calculations for S_N2 reactions overestimate the solution-phase barrier by only 2 kcal mol^{-1}, confirming the accuracy of the continuum model for ionic reactions in dipolar aprotic solvents, as anticipated from extensive pK_a calculations [130].

In the case of protic solvents such as water, the continuum models are less accurate, especially for small ions or those with highly localized partial charges because of the importance of specific solute–solvent interactions in the first solvation shell [115, 132]. As an example, Pliego and Riveros [152] investigated the hydroxide ion addition to ethyl acetate in aqueous solution to form a tetrahedral intermediate. They used the PCM method with only electrostatic contributions. The liquid-phase free energy barrier for this step, calculated at MP2/6-311+G(2df,2p)//HF/6-31+G(d) level of electronic structure theory is 17.6 kcal mol^{-1}, while the experimental value is 18.8 kcal mol^{-1}. The small error is due to overestimation of the barrier by the MP2 calculations. In a similar system [158], MP4 calculations decrease the barrier by 2 kcal mol^{-1} in relation to MP2 energies. Thus, using more reliable gas-phase energies should lead to an underestimation of the barrier by about 3 kcal mol^{-1}. In addition, liquid-phase optimization could produce an even smaller barrier, increasing the deviation.

The studies just reviewed were based on geometries optimized in the gas phase, and the nonbulk electrostatic contributions were not included. However these refinements

are included in some other work. As an example, Kormos and Cramer [144] have investigated the identity S_N2 reaction $H_2C=CHCH_2Cl+Cl^-$ in aqueous solution using DFT calculations and the SM5.42 method. Optimizations were done for both gas phase and solution in order to evaluate the solvent effect on the transition state structure and free energy. They found that liquid-phase optimization decreases the barrier by 1.5 kcal mol^{-1} in this case, and the gas-phase and liquid-phase geometries were reasonably close. In contrast, for the identity $(CH_3)_2C=CHCH_2Cl+Cl^-$ reaction, the barrier dropped by 6 kcal mol^{-1}, and a large difference was found between the geometry in aqueous solution and the gas-phase geometry. This behavior can be explained if we consider that in the latter case, the transition state resembles a stable tertiary carbocation species, allowing both of the chlorine atoms to be more distant from the carbon atom for the liquid-phase transition state structure. Systems with solvent-dependent transition states include amide hydrolysis [153] and decarboxylations [154]. Such effects are sometimes studied by microhydration models [155–157]. It is expected that in DMSO and other dipolar aprotic solvents, liquid-phase optimization should be less important than in aqueous solution.

The united atom for Hartree–Fock (UAHF) method [135] uses environment-dependent, charge-dependent atomic radii in order to try to improve the accuracy of continuum solvation calculations, but this has not always worked well. An example is the identity $Cl^- + CH_3Cl \rightarrow ClCH_3 + Cl^-$ reaction in aqueous solution. Vayner *et al.* [145] have studied this symmetrical S_N2 reaction using the CPCM model with the UAHF parametrization. The gas-phase energies were determined at the CBS-QB3 level. The calculated free energy of activation was 35.3 kcal mol^{-1}, a very high value. They found that the solvent contribution to the barrier is 27.3 kcal mol^{-1}, which can be compared with an estimated experimental value of $\sim$ 23 kcal mol^{-1}. For the same system, Truong and Stefanovich [142] used the GCOSMO method to study these identity reactions in aqueous solution. In their calculations, the solvent contribution to the free energy of activation is in the range of 17–19 kcal mol^{-1}, depending on the *ab initio* method used.

The lower reliability of the continuum models for modeling ionic reactions in situations where there are strong solute–solvent interactions can be partially overcome by introducing some explicit solvent molecules, as in the cluster–continuum model [116]. Two interesting systems that have been studied using this approach are the basic hydrolyses of methyl formate [158] and formamide [159]. An extensive analysis of the different reaction pathways of methyl formate was carried out. The free energy of activation profile for all the pathways was obtained at the MP4/6-311+G(2df,2p)/HF/6-31+G(d) level of electronic structure theory combined with the cluster–continuum model, where the IPCM method was used for the continuum electrostatics. Pliego and Riveros [158] calculated that the direct attack of the hydroxide ion on the carbonyl group, leading to a tetrahedral intermediate, has a free energy of activation of 15.2 kcal mol^{-1}, in good agreement with the experimental value of 15.3 kcal mol^{-1}. In addition, another reaction pathway was investigated, where the water molecule hydrating the hydroxide ion acts as the attacking species, and the hydroxide ion acts as a general base. Both the transition states for these pathways are presented in Figure 3.11. The free energy barrier for this general base catalysis mechanism was calculated to be 16.3 kcal mol^{-1}, indicating that this mechanism is less important. Therefore, the calculations resolved the experimental

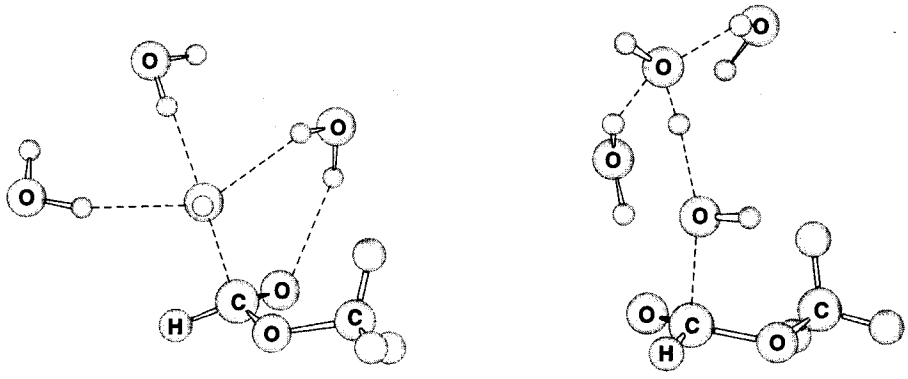

Figure 3.11 *Application of the cluster–continuum model for basic hydrolysis of the methyl formate.*

controversy [160] about the true reaction mechanism, indicating that the direct hydroxide ion attack is the most important pathway, although some products are generated from the coordination-water attack pathway. On the other hand, in the case of basic hydrolysis of formamide, Pliego [159] found that only the direct hydroxide ion attack can take place. This finding obtained using the cluster–continuum model, was recently confirmed by an explicit-solvation molecular dynamics study by Blumberger and co-workers [161, 162], where no coordination-water attack mechanism was found.

A review [86] written in 1998 already gave 17 references for transition state geometries optimized in solution; this is particularly straightforward when stable analytic gradients [113, 163] are available. Liquid-phase optimization can be very important in some reactions. In Figure 3.8, although the relative energy of the stationary points changes due to solvation, gas-phase structures provide a good approximation. The situation is different for neutral–neutral S_N2 reactions such as the example $NH_3 + CH_3Cl \rightarrow NH_3CH_3^+ + Cl^-$. The formation of two charged species has a large solvent effect, and the $N-C$ and $C-Cl$ distances in the transition state must be determined under liquid-phase conditions [32, 164–167]. However, SES and ESP models produce very similar free energy profiles as a function of $R_b - R_f - (R_b - R_f)^{\ddagger}$, where R_b is the breaking bond distance, and R_f is the forming bond distance [32].

Even more important than changing the geometries, in some cases the solvent can induce a different electronic structure than in the gas phase process, leading to a new reactive process. A very interesting example is the halogenation of alkenes [168–176] or alkynes [177, 178]. Figure 3.12 illustrates the products generated in an apolar solvent and in polar solvents. In low-polarity solvents, chlorination takes place through a radical mechanism [177], while in polar solvents, the stabilization of the charged species favors the ionic mechanism. In the case of bromination, the ionic mechanism also occurs in polar solvents [168, 171]. However, in apolar solvents, a second bromine molecule can participate of the process, forming the tribromide ion [168, 171].

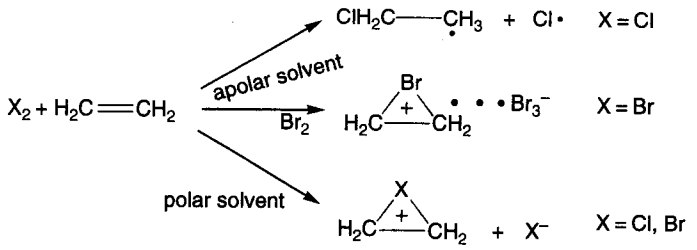

Figure 3.12 *Halogenation in apolar and polar solvents.*

The halogenation reaction of ethylene has been modeled by many researchers [170, 172–176]. For chlorination in apolar solvents (or in the gas phase), the formation of two radical species requires the use of flexible CASSCF and MRCI electronic structure methods, and such calculations have been reported by Kurosaki [172]. In aqueous solution, Kurosaki has used a mixed discrete–continuum model to show that the reaction proceeds through an ionic mechanism [174]. The bromination reaction has also received attention [169, 170]. However, only very recently was a reliable theoretical study of the ionic transition state using PCM/MP2 liquid-phase optimization reported by Cammi *et al.* [176]. These authors calculated that the free energy of activation for the ionic bromination of the ethylene in aqueous solution is 8.2 kcal mol^{-1}, in good agreement with the experimental value of 10 kcal mol^{-1}.

Xie *et al.* [179] calculated the free energies of reaction and activation in the gaseous and liquid phase for the following aryl ester hydrolysis reaction: His... H_2O... $MeC(O)OC_6H_4CH_3$ → His... $HOC_6H_4CH_3$ + $MeC(O)OH$. In the gas phase they obtained a free energy of reaction $\Delta G^\circ = -4.5$ kcal mol^{-1} and a free energy of activation $\Delta G^{\ddagger,\circ}$ of 44.3 kcal mol^{-1}. Solvation has only a small effect on ΔG°; PCM implicit solvent calculations yield −6.6 kcal mol^{-1} in $HCCl_3$ and −8.0 kcal mol^{-1} in H_2O. However the transition state has considerable zwitterionic character and PCM calculations lower $\Delta G^{\ddagger,\circ}$ to 27.6 kcal mol^{-1} in $HCCl_3$ and 16.1 kcal mol^{-1} in H_2O, which is consistent with experiment [180].

Rod *et al.* [181] compared continuum and discrete solvation models for the reaction by which $S(CH_3)_3^+$ transfers a methyl group to an oxygen of a catecholate ligated to Mg^{2+}. The gas-phase reaction, which is calculated to be exoergic by 53 kcal mol^{-1}, was calculated to occur without a barrier. In solution, a simulation with 8800 T1P3P explicit solvent molecules yielded a reaction exoergicity of 21 kcal mol^{-1} and a free energy of activation of 13.1 kcal mol^{-1}. Four implicit solvation models yielded free energies of activation of 10.9, 11.2, 12.7, and 13.9 kcal mol^{-1}, in reasonable agreement with the explicit-solvent calculation.

Although enzyme catalysis has usually been modeled with discrete solvent models [2, 182], Rod *et al.* [181] also performed an interesting comparison of discrete and continuum models for the methyl transfer from *S*-adenosylmethione to catecholate catalyzed by catechol *O*-methyltransferase. In this case the protein was explicit in both simulations, one with 7800 T1P3P water molecules and two others with implicit solvent, each having different atomic radii. The explicit calculation gave a free energy of activation of 16.3 kcal mol^{-1}, and the implicit ones both gave 15.5 kcal mol^{-1}. It is not surprising

that the implicit models are better for the enzyme reaction than the aqueous nonenzymatic reaction because the solvent is not interacting strongly with the reactants. A troubling result is that there are more protein hydrogen bonds and salt bridges in the implicit simulation than in the explicit one, but not all the hydrogen bonds and salt bridges of the explicit simulation are preserved in the implicit one. This kind of difference is highlighted in earlier studies [183–185] of protein dynamics where explicit and implicit solvent models were compared, and implicit models were found to be less accurate.

Another comparison of discrete and continuum molecules was carried out for the decarboxylation of 4-pyridylacetic acid zwitterion in aqueous solution [157]. Transition states were optimized with the SM5.42 implicit solvation model with zero, one, or two discrete water molecules, yielding free energies of activation of 24.2, 21.2, and 18.3 kcal mol^{-1}, respectively, as compared to -4.7 kcal mol^{-1} in the gas phase. The fact that one can obtain quite different solvation free energies for ions without and with discrete solvent is not surprising in light of the discussion in Section 3.3.3. Including only two discrete waters without the continuum yields $\Delta G^{\ddagger} = +1.1$ kcal mol^{-1}, very far from the results with implicit solvent, which again is not surprising since one expects that ionic solvation energies converge very slowly as solvent molecules are added. Kinetic isotope effects for this reaction were found to be less sensitive than $\Delta G^{\ddagger}$ to the inclusion of solvation effects.

An important prototype reaction where both discrete and continuum solvation models have been applied is the Claisen rearrangement of allyl vinyl ether to 4-pentenal. This is an electrocyclic reaction proceeding by a [3,3] sigmatropic shift, and the interpretation of solvent effects is complicated by the difficulty of modeling the polarity of the transition state even in the gas phase, as reviewed elsewhere [186]. Severance and Jorgensen [187,188] provided the first correct account of the solvation effects on the basis of explicit-solvent calculations. Their calculated rate acceleration in aqueous solution, relative to the gas phase, corresponds to a lowering of $\Delta G^{\ddagger,o}$ by 3.8 kcal mol^{-1}, which may be compared to a lowering of 4.0 that they estimated from various experiments. The acceleration was attributed to enhanced hydrogen bonding at the transition state. A later explicit-solvent calculation by Gao [189] gave a lowering of 3.5 kcal mol^{-1}. Earlier predictions [190] by implicit-solvent models gave much smaller effect, 0.7 kcal mol^{-1}, but that is now attributed to inaccurate modeling of the charge distribution at the transition state in the early studies. Using a more accurate charge distribution based on MCSCF electronic structure calculations gave a lowering of $\Delta G^{\ddagger,o}$ of 4.3 kcal mol^{-1} [186]. These results indicate the high sensitivity of predicted solvent effects on rate constants to getting the charge distributions right in solution by self-consistent reaction fields. They also show that continuum models can sometimes account well for hydrogen bonding effects.

Although ionic mechanisms are more common in aqueous solution than radical mechanisms, Nguyen and co-workers [191] presented an interesting application of continuum solvation models to a radical reaction, in particular $CH_3 + H_2O_2 \rightarrow CH_4 + HO_2$, in aqueous solution. They used the PCM/HF/6-31G** continuum solvation model, with UAHF radii and including electrostatics, cavitation, dispersion, and repulsion, to calculate the standard-state free energy of solvation of the transition state to be -5.4 kcal mol^{-1} and that of reactants to be -9.4 kcal mol^{-1}, with the difference being $+4.1$ kcal mol^{-1}.

A similar calculation with the COSMO–RS solvation model gave $-4.7\,\mathrm{kcal\,mol^{-1}}$ for the transition state, $-7.2\,\mathrm{kcal\,mol^{-1}}$ for reactants, and $+2.5\,\mathrm{kcal\,mol^{-1}}$ for the difference. Experimentally, it is found that the reaction rate is 1.2×10^3 times slower in aqueous solution than in the gas phase [192], corresponding to an increase in the free energy of activation of $4.2\,\mathrm{kcal\,mol^{-1}}$, in excellent agreement with PCM ($4.1\,\mathrm{kcal\,mol^{-1}}$) but not with COSMO–RS ($2.5\,\mathrm{kcal\,mol^{-1}}$). The good agreement with PCM was attributed to successful parameterization. The solvation difference of the transition state from reactants was found to be very close (0.2–$0.3\,\mathrm{kcal\,mol^{-1}}$) to the difference between that for products and that for reactants in this reaction. This is curious because the reaction is exothermic, and the transition state breaking and forming bond distances are (as expected from the Hammond postulate) more reactant-like than product-like, although the O – O – H bond angle is more product-like.

Another application of continuum models to radical reactions is provided by the hydrogen abstracton $H + CH_3OH \rightarrow H_2 + CH_2OH$ [61,193], for which experimental [194, 195] kinetic isotope effects are available. These studies [166,193] also include variational effects, multidimensional tunneling, nonequilibrium solvation, and kinetic isotope effects, as well as the coupling between these effects. Including an optimized multidimensional treatment of tunneling, the ESP rate constant for the perprotio reaction is 2.0 times larger than the SES one, and the NES rate constant is 52 % smaller than the ESP one for the 'best' nonequilibrium solvation parameters. The comparison of aqueous-phase and gas-phase rate constants needs to be re-examined now because the gas-phase transition state is now better understood [196] than when the liquid-phase study was conducted.

The 1,2-hydride shift in phenyl glyoxal hydrate to produce mandelate and the corresponding deuteride shift have been studied using continuum solvation models and VTST with multidimensional tunneling by Tresadern *et al.* [197]. They found that, starting from a reaction intermediate, the varational effect lowers the overbarrier rate constant k by 26 % and kinetic isotope effect (KIE) by 6 %. Tunneling, in contrast, raises k by a factor of 5.1 and the KIE by 71 %. Without corner cutting, the tunneling effect would be much smaller (factor of 3.6 and 51 %, respectively).

A challenging test of all kinds of models of liquid-phase reaction rates is provided by the measurement of six different kinetic isotope effects (two secondary H/D at different positions, one $^{11}C/^{14}C$, and $^{12}C/C^{13}$ at a different position, one $^{14}N/^{14}N$, and one $^{35}Cl/^{37}Cl$) for the S_N2 reaction between $(n-C_4H_9)_4NCN$ and C_2H_5Cl in dimethylsulfoxide at 303 K [145]. The mean of the unsigned deviations from unity these six KIEs. The experimental values of these KIEs are 0.990, 1.014, 1.21, 1.001, 1.000, and 1.007. All KIEs will then be calculated by transition state theory. In the same order, the best theoretical method, based on B3LYP/aug-cc-pVDZ gas-phase electronic structure calculations gave 0.994, 1.005, 1.17, 0.993, 1.000, and 1.007, which is very good for five of the six results. Adding solvation by the PCM/UAHF method yielded 0.973, 0.978, 1.17, 0.993, 1.000, and 1.007 (in the same order), which is less accurate in half the cases. Probably the conclusion to be drawn is that solvent effects are small, and the error is dominated more by the quality of the electronic structure theory than the quality of the solvation model. In some cases, the solvent effect on rate constants has been carefully investigated by continuum models, and it has been found to be small [198, 199].

Continuum solvation models have also been used to rationalize the Hammett ρ^+ parameters determined [200] from S_N1 solvolysis rate constants [201] of cumyl chlorides. In particular the SM5.42R/AM1 [112] model reproduces the experimental ρ^+ within 24 %. The use of continuum models for placing the empirical correlations of physical organic chemistry on a firmer basis is in its infancy.

3.3.5 Competitive Reactions

Many important chemical reactions have competitive parallel pathways. In some cases, this competition is very significant and can diminish the yield of desired product. The ability to predict branching ratios is helpful for planning synthetic routes, and as a consequence, an important goal of theoretical studies of chemical reactions is to be able to predict the product ratio.

An interesting system where parallel pathways play an important role is the S_N2 nitration of alkyl halides (Figure 3.13). The nucleophilic attack of the nitrite ion can take place through the nitrogen, leading to nitroalkanes, or through the oxygen atom, producing the alkyl nitrite. Nitroalkanes are the desired products due to their importance as well as their utilization as chemical intermediates to further transformation. In the case of the reaction of the nitrite ion with *n*-hepthyl bromide, experimental studies show that only 67 % of the product is the nitroalkane, and a large amount of the alkyl nitrite (33 %) is formed [202].

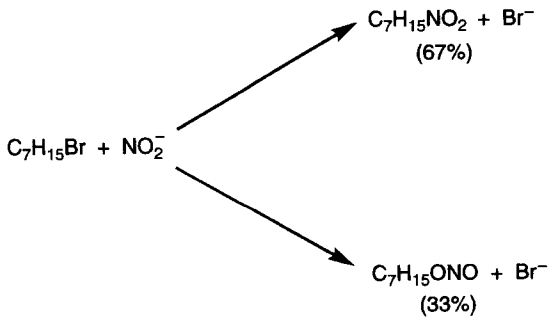

Figure 3.13 *Experimental product ratio in the S_N2 reaction of n-hepthyl bromide with nitrite ion in dimethyl formamide (DMF) solution.*

Westphal and Pliego [203] have recently performed a high-level *ab initio* study of the prototypical system $CH_3CH_2Br + NO_2^-$, which is a good representation of the *n*-hepthyl bromide reaction. Gas-phase geometry optimizations were done at the MP2/6-31+G(d) level of electronic structure theory, followed by single-point energy calculations at the CCSD(T)/6-311+G(2df,2p) level (for bromine, Ahlrichs' TZVPP basis set was used) and solvent contribution at PCM/B3LYP/6-31+G(d) level (DMSO solvent, Pliego and Riveros parametrization). Using transition state theory, they predicted that the nitroalkane and alkyl nitrite are formed in the proportion of 46:54, in good agreement with the experimental data for the hepthyl bromide, 67:33. This shows that continuum solvation models can be very useful for application in synthetic chemistry.

3.3.6 Catalyst Design and Control of Chemical Reactions

Our present ability for modeling chemical processes using theoretical methods constitutes a very powerful tool in the design of new catalysts. Continuum solvation models have been used in the design and modeling of metallocene catalysts for olefin polymerization [204, 205] and Pd(II) ligand systems to perform aerobic oxidations of secondary alcohols [206].

Continuum solvation models have been used in the design of a novel supramolecular organocatalytic concept, aimed to selectively stabilize S_N2 transition states [148,150,207]. Such development can become a very useful tool for controlling the regioselectivity, chemoselectivity, and enantioselectivity of S_N2 reactions. It should also be mentioned that the solvent itself may be considered a catalyst [101–103, 153, 208–210].

3.3.7 Conclusion

Continuum solvation models can be used to predict the free energy of activation of chemical reactions and the effective potential for condensed-phase tunneling, and they can therefore be combined with transition state theory to predict chemical reaction rates.

Acknowledgments

D.G.T. is grateful to Christopher J. Cramer, Jiali Gao, Bruce C. Garrett, Gregory K. Schenter, and many students and postdoctoral research associates for collaboration on innumerable solvation projects. This work was supported in part by the National Science Foundation under grant no. CHE03-49122.

J.R.P.Jr. thanks Professors Jose M. Riveros, Stella M. Resende and Wagner B. de Almeida, and students Gizelle I. Almerindo, Daniel W. Tondo and Eduard Westphal for collaborative work. He is also grateful to the Brazilian Research Council (CNPq, Profix program) for the support.

References

[1] M. M. Kreevoy and D. G. Truhlar, in C. Bernasconi (ed.), *Investigation of Rates and Mechanisms of Reactions*, Vol. 6 of A. Weissberger (ed.) *Techniques of Chemistry*, 4th edn, John Wiley & Sons, Inc., New York, Part I, 1986, pp 13–95.
[2] M. Garcia-Viloca, J. Gao, M. Karplus and D. G. Truhlar, *Science*, **303** (2004) 186.
[3] K. A. Holbrook, M. J. Pilling and S. H. Robertson, *Unimolecular Reactions*, John Wiley & Sons, Ltd, Chichester, 1996.
[4] D. G. Truhlar, B. C. Garrett and S. J. Klippenstein, *J. Phys. Chem.*, **100** (1996) 12771.
[5] M. Lee, G. R. Holtom and R. M. Hochstrasser, *Chem. Phys. Lett.*, **118** (1985) 359.
[6] M. A. Wilson and D. Chandler, *J. Phys. Chem.*, **149** (1990) 11.
[7] J.-M. Depaepe and J.-P. Ryckaert, *Chem. Phys. Lett.*, **245** (1995) 653.
[8] S. H. Courtney and G. R. Fleming, *Chem. Phys. Lett.*, **103** (1984) 443.
[9] J. Hicks, M. Vandersall, Z. Barbarogis and K. B. Eisenthal, *Chem. Phys. Lett.*, **116** (1985) 18.
[10] E. Wigner, *Trans. Faraday Soc.*, **34** (1938) 29.
[11] J. C. Keck, *J. Chem. Phys.*, **32** (1960) 1035.
[12] J. B. Anderson, *Adv. Chem. Phys.*, **91** (1995) 381.

[13] H. S. Johnston, *Gas Phase Reaction Rate Theory*, Ronald Press, New York, 1966, pp 122–128.
[14] B. H. Mahan, *J. Chem. Educ.*, **51** (1974) 709.
[15] A. Ma and A. R. Dinner, *J. Phys. Chem. B*, **109** (2005) 6769.
[16] S. Consta, *Theor. Chem. Acc.*, **116** (2006) 373.
[17] B. Ensing, M. D. Vivo, Z. Liu, P. Moore and M. L. Klein, *Acc. Chem. Res.*, **39** (2006) 73.
[18] C. K. Schenter, B. C. Garrett and D. G. Truhlar, *J. Chem. Phys.*, **119** (2003) 5828.
[19] P. Atkins and R. S. Friedman, *Molecular Quantum Mechanics*, 4th edn, Oxford University Press, Oxford, 2005, pp 250–251.
[20] P. Pechukas, *Ber. Bunsenges. Phys. Chem.*, **86** (1982) 372.
[21] B. C. Garrett and D. G. Truhlar, *J. Chem. Phys.*, **70** (1979) 1593.
[22] D. G. Truhlar and B. C. Garrett, *Acc. Chem. Res.*, **13** (1980) 440.
[23] D. G. Truhlar and B. C. Garrett, *Annu. Rev. Phys. Chem.*, **35** (1984) 159.
[24] B. C. Garrett and D. G. Truhlar, in P. v. R. Schleyer, N. L. Allinger, T. Clark, J. Gasteiger, P. A. Kollman and H. F. Schaefer III (eds), *Encyclopedia of Computational Chemistry*, Vol. 5, John Wiley & Sons, Ltd, Chichester, pp 3094–3104.
[25] B. C. Garrett and D. G. Truhlar, in C. Dykstra, G. Frenking, K. S. Kim and G. E. Scuseria (eds), *Theory and Applications of Computational Chemistry: The First Forty Years*, Elsevier, Ltd, Amsterdam, 2005, pp 67–87.
[26] D. G. Truhlar, J. Gao, M. Garcia-Viloca, C. Alhambra, J. Corchado, M. L. Sanchez and T. D. Poulsen, *Int. J. Quantum Chem.*, **100** (2004) 1136.
[27] D. G. Truhlar, in A. Kohen and H.-H. Limbach (eds), *Isotope Effects in Chemistry and Biology*, Taylor and Francis, Boca Raton, FL, 2006, pp 579–619.
[28] S. C. Tucker, in P. Talkner and P. Hänggi, Understanding Chemical Reactivity Series (eds), *New Trends in Kramers' Reaction Rate Theory*, Vol. 11, Kluwer, Dordrecht, 1995, pp 5–46.
[29] Ref. 1, pp. 46–49.
[30] B. C. Garrett and G. K. Schenter, *Int. Rev. Phys. Chem.*, **13** (1994) 263.
[31] D. G. Truhlar, Y.-P. Liu, G. K. Schenter and B. C. Garrett, *J. Phys. Chem.*, **98** (1994) 8396.
[32] Y. Y. Chuang, C. J. Cramer and D. G. Truhlar, *Int. J. Quantum Chem.*, **70** (1998) 887.
[33] Y.-P. Liu, D.-h. Lu, A. González-Lafont, D. G. Truhlar and B. C. Garrett, *J. Am. Chem. Soc.*, **115** (1993) 7806.
[34] A. Fernandez-Ramos and D. G. Truhlar, *J. Chem. Phys.*, **114** (2001) 491.
[35] H. Eyring, *J. Chem. Phys.*, **3** (1935) 107.
[36] D. G. Truhlar, A. D. Isaacson and B. C. Garrett, in M. Baer (eds), *Theory of Chemical Reaction Dynamics*, Vol. 4, CRC Press, Boca Raton, FL, 1985, pp 65–137.
[37] W. F. K. Wynne-Jones and H. Eyring, *J. Chem. Phys.*, **3** (1935) 492.
[38] M. G. Evans, *Trans. Faraday Soc.*, **34** (1938) 49.
[39] D. G. Truhlar and A. Kuppermann, *J. Am. Chem. Soc.*, **93** (1971) 1840.
[40] B. C. Garrett and D. G. Truhlar, *J. Phys. Chem.*, **112** (1979) 1079.
[41] R. A. Marcus, *J. Chem. Phys.*, **49** (1968) 2610.
[42] I. Shavitt, *J. Chem. Phys.*, **49** (1968) 4048.
[43] K. Fukui, *Acc. Chem. Res.*, **14** (1981) 363.
[44] B. C. Garrett and D. G. Truhlar, *J. Phys. Chem.*, **83** (1979) 1052.
[45] A. D. Isaacson and D. G. Truhlar, *J. Chem. Phys.*, **76** (1982) 1380.
[46] C. F. Jackels, Z. Gu and D. G. Truhlar, *J. Chem. Phys.*, **102** (1995) 3188.
[47] Y.-Y. Chuang and D. G. Truhlar, *J. Phys. Chem. A*, **102** (1998) 242.
[48] J. Villà and D. G. Truhlar, *Theor. Chem. Acc.*, **97** (1997) 317.
[49] P. L. Fast, J. C. Corchado and D. G. Truhlar, *J. Chem. Phys.*, **109** (1998) 6237.
[50] P. L. Fast and D. G. Truhlar, *J. Chem. Phys.*, **109** (1998) 3721.

[51] B. C. Garrett and D. G. Truhlar, *J. Phys. Chem.*, **83** (1979) 2921.
[52] D. G. Truhlar and A. Kupperman, *Chem. Phys. Lett.*, **9** (1971) 269.
[53] D.-h. Lu, T. N. Truong, V. S. Melissas, G. C. Lynch, Y.-P. Liu, B. C. Garrett, R. Steckler, A. D. Isaacson, S. N. Rai, G. C. Hancock, J. G. Lauderdale, T. Joseph and D. G. Truhlar, *Comput. Phys. Commun.*, **71** (1992) 235.
[54] T. N. Truong, D.-h. Lu, G. C. Lynch, Y.-P. Liu, V. S. Melissas, J. J. P. Stewart, R. Steckler, B. C. Garrett, A. D. Isaacson, A. Gonzàlez-Lafont, S. N. Rai, G. C. Hancock, T. Joseph and D. G. Truhlar, *Comput. Phys. Commun.*, **75** (1993) 143.
[55] Y.-P. Liu, G. C. Lynch, T. N. Truong, D.-h. Lu, D. G. Truhlar and B. C. Garrett, *J. Am. Chem. Soc.*, **115** (1993) 2408.
[56] T. C. Allison and D. G. Truhlar, in D. L. Thompson (eds), *Modern Methods for Multidimensional Dynamics Computations in Chemistry*, World Scientific, Singapore, 1998, pp 618–712.
[57] J. Pu and D. G. Truhlar, *J. Chem. Phys.*, **117** (2002) 1479.
[58] W. L. Jorgensen, *Acc. Chem. Res.*, **22** (1989) 184.
[59] A. J. Parker, *Chem. Rev.*, **69** (1969) 1.
[60] B. C. Garrett and G. K. Schenter, in C. J. Cramer and D. G. Truhlar (eds), *Structure and Reactivity in Aqueous Solution*, ACS Symp. Ser. 568, American Chemical Society, Washington, DC, 1994, pp 122–142.
[61] Y.-Y. Chuang and D. G. Truhlar, *J. Am. Chem. Soc.*, **121** (1999) 10157.
[62] S. Lee and J. T. Hynes, *J. Chem. Phys.*, **88** (1988) 6853.
[63] E. Pollak, S. C. Tucker and B. J. Berne, *Phys. Rev. Lett.*, **65** (1990) 1399.
[64] G. K. Schenter, R. P. McRae and B. C. Garrett, *J. Chem. Phys.*, **97** (1992) 9116.
[65] D. G. Truhlar, G. K. Schenter and B. C. Garrett, *J. Chem. Phys.*, **98** (1993) 5756.
[66] M. V. Basilevsky, G. E. Chudinov and D. V. Napolov, *J. Phys. Chem.*, **97** (1993) 3270.
[67] M. F. Ruiz-López, A. Oliva, I. Tuñón and J. Bertrán, *J. Phys. Chem. A*, **102** (1998) 10728.
[68] D. G. Truhlar and B. C. Garrett, *J. Phys. B*, **104** (2000) 1069.
[69] C. J. Cramer and D. G. Truhlar, in M. R. Reddy and M. D. Erion (eds), *Free Energy Calculations in Rational Drug Design*, Kluwer, Plenum, New York, 2001, pp 63–95.
[70] G. K. Schenter, B. C. Garrett and D. G. Truhlar, *J. Phys. Chem. B*, **105** (2001) 9672.
[71] S. A. Adelman and J. D. Doll, *J. Chem. Phys.*, , **64** (1976) 2375.
[72] T. F. George, K.-T. Lee, W. C. Murphy, M. Hutchinson and H.-W. Lee, in M. Baer (eds), *Theory of Chemical Reaction Dynamics*, Vol. 4, CRC Press, Boca Raton, FL, 1985, pp 139–169.
[73] J. T. Hynes, in M. Baer (eds), *Theory of Chemical Reaction Dynamics*, Vol. 4, CRC Press, Boca Raton, FL, 1985, pp 171–234.
[74] J. T. Hynes, in J. D. Simon (eds), *Ultrafast Dynamics of Chemical Systems*, Understanding Chemical Reactivity Series, Vol. 7, Kluwer, Dordrecht, 1994, pp 345–381.
[75] R. Zwanzig, *Nonequilibrium Statistical Mechanics*, Oxford University Press, New York 2001.
[76] M. Maroncelli and G. R. Fleming, *J. Chem. Phys.*, **89** (1988) 5044.
[77] J. Faeder and B. M. Ladanyi, *J. Phys. Chem. B*, **105** (2001) 11148.
[78] M. J. Bedard-Hearn, R. G. Larsen and B. J. Schwartz, *J. Phys. Chem. B*, **107** (2003) 14464.
[79] F. Ingrosso, B. M. Ladanyi, B. Mennucci, M. D. Elola and J. Tomasi, *J. Phys. Chem. B*, **109** (2005) 3553.
[80] G. van der Zwan and J. T. Hynes, *J. Chem. Phys.*, **76** (1982) 2993.
[81] B. Bagchi, D. W. Oxtoby and G. R. Fleming, *Chem. Phys.*, **86** (1984) 257.
[82] D. Zichi and J. T. Hynes, *J. Chem. Phys.*, **88** (1988) 2513.

[83] Y. Lin and C. D. Jonah, in J. D. Simon (eds), *Ultrafast Dynamics of Chemical Systems*, Understanding Chemical Reactivity Series, Vol. 7, Kluwer & Sons, Ltd, Dordrecht, 1994, pp 137–162.
[84] B. J. Gertner, K. Ando, R. Bianco and J. T. Hynes, *Chem. Phys.*, **183** (1994) 309.
[85] J. R. Mathis and J. T. Hynes, *J. Phys. Chem.*, **98** (1994) 5445.
[86] C. J. Cramer and D. G. Truhlar, *Chem. Rev.*, **99** (1999) 2161.
[87] D. G. Truhlar, J. Gao, C. Alhambra, M. Garcia-Viloca, J. Corchado, M. L. Sánchez and J. Villà, *Acc. Chem. Res.*, **35** (2002) 341.
[88] M. A. Aguilar, F. J. Olivares del Valle and J. Tomasi, *J. Chem. Phys.*, **98** (1993) 7375.
[89] M. L. Sánchez, M. A. Aguilar and F. J. Olivares del Valle, *J. Phys. Chem.*, **99** (1995) 15758.
[90] K. V. Mikkelson, A. Cesar, A. Ågren and H. J. A. Jensen, *J. Chem. Phys.*, **103** (1995) 9010.
[91] M. F. Ruiz-López, D. Rinaldi and J. Bertrán, *J. Chem. Phys.*, **103** (1995) 9249.
[92] X. Assfeld, J. Garapon, D. Rinaldi, M. F. Ruiz-López and J. L. Rivail, *J. Mol. Struc. Theorchem.*, **271** (1996) 107.
[93] B. Mennucci, R. Cammi and J. Tomasi, *J. Chem. Phys.*, **107** (1998) 2798.
[94] J. Li, C. J. Cramer and D. G. Truhlar, *Int. J. Quantum Chem.*, **77** (2000) 264.
[95] F. R. Tortunda, E. Silla, I. Tuñón, D. Rinaldi and M. F. Ruiz-López, *Theor. Chem. Acc.*, **104** (2000) 89.
[96] M. Cossi and V. Barone, *J. Chem. Phys.*, **112** (2000) 2427.
[97] M. Cossi and V. Barone, *J. Chem. Phys.* A, **104** (2000) 10614.
[98] R. Karmacharya, D. Antoniou and S. D. Schwartz, *J. Phys. Chem. A*, **105** (2001) 2563.
[99] X.-Y. Li and K.-X. Fu, *J. Theor. Comput. Chem.*, **4** (2005) 907.
[100] K.-X. Fu, Q. Zhu, X.-Y. Li, Z. Gong, J.-Y. Ma and R.-X. He, *J. Comput. Chem.*, **27** (2005) 368.
[101] T. Yamabe, K. Yamashita, M. Kaminoyama, M. Koizumi, A. Tachibana and K. Fukui, *J. Phys. Chem.*, **88** (1984) 1459.
[102] K. A. Nguyen, M. S. Gordon and D. G. Truhlar, *J. Am. Chem. Soc.*, **113** (1991) 1596.
[103] M. T. Nguyen, G. Raspoet and L. G. Vanquickenborne, *J. Am. Chem. Soc.*, **119** (1997) 2552.
[104] R. K. Wangsness, *Electromagnetic Fields*, John Wiley & Sons, Inc., New York; 1979, pp. 179ff.
[105] A. C. Muskun, A. E. Jailaubekov, S. E. Bradforth, G. Tao and R. M. Stratt, *Science*, **311** (2006) 1907.
[106] O. Curuchet, C. J. Cramer, D. G. Truhlar, M. F. Ruiz-Lopez, M. Orozco and F. J. Luque, *J. Comput. Chem.*, **24** (2003) 284.
[107] C. J. Cramer and D. G. Truhlar, in G. Maroulis and T. E. Simos (eds), *Trends and Perspectives in Modern Computational Science*, Vol. 6, Brill/VSP, Leiden, 2006, pp. 112–140.
[108] C. C. Chambers, G. D. Hawkins, C. J. Cramer and D. G. Truhlar, *J. Phys. Chem.*, **100** (1996) 16385.
[109] D. J. Giesen, G. D. Hawkins, D. A. Liotard, C. J. Cramer and D. G. Truhlar, *Theor. Chem. Acc.*, **98** (1999) 85, **101** (1997) 309(E).
[110] G. D. Hawkins, C. J. Cramer and D. G. Truhlar, *J. Phys. Chem. B*, **102** (1998) 3257.
[111] T. Zhu, J. Li, G. D. Hawkins, C. J. Cramer and D. G. Truhlar, *J. Chem. Phys.*, **109** (1998) 9117; **111** (1999) 5624(E); **113** (2000) 3930(E).
[112] J. Li, T. Zhu, G. D. Hawkins, P. Winget, D. A. Liotard, C. J. Cramer and D. G. Truhlar, *Theor. Chem. Acc.*, **103** (1999) 9.
[113] T. Zhu, J. Li, D. A. Liotard, C. J. Cramer and D. G. Truhlar, *J. Chem. Phys.*, **110** (1999) 5503.
[114] J. D. Thompson, C. J. Cramer and D. G. Truhlar, *J. Phys. Chem. A*, **108** (2004) 6532.
[115] C. P. Kelly, C. J. Cramer and D. G. Truhlar, *J. Chem. Theory Comput.*, **1** (2005) 1133.
[116] J. R. Pliego Jr. and J. M. Riveros, *J. Phys. Chem. A*, **105** (2001) 7241.
[117] C. P. Kelly, C. J. Cramer and D. G. Truhlar, *J. Phys. Chem. A*, **110** (2006) 2493.

[118] L. R. Pratt and R. A. Laviolette, *Mol. Phys.*, **94** (1998) 909.
[119] D. Asthagiri and L. R. Pratt, *Chem. Phys. Lett.*, **371** (2003) 613.
[120] D. Asthagiri, L. R. Pratt and J. D. Kress, *Chem. Phys. Lett.*, **380** (2003) 530.
[121] D. Asthagiri, L. R. Pratt and H. S. Ashbaugh, *J. Chem. Phys.*, **119** (2003) 2702.
[122] D. Asthagiri, L. R. Pratt, M. E. Paulaitis and S. B. Rempe, *J. Am. Chem. Soc.*, **126** (2004) 1285.
[123] E. Wesphal and J. R. Pliego Jr., *J. Chem. Phys.*, **123** (2005) 74508.
[124] R. G. Pearson, *J. Am. Chem. Soc.*, **108** (1986) 6109.
[125] J. R. Pliego, Jr. and J. M. Riveros, *Chem. Phys. Lett.*, **332** (2000) 597.
[126] J. R. Pliego, Jr. and J. M. Riveros, *Phys. Chem. Chem. Phys.*, **4** (2002) 1622.
[127] C. P. Kelly, C. J. Cramer and D. G. Truhlar, *J. Phys. Chem. B*, **111** (2007) 408.
[128] J. R. Pliego, Jr. and J. M. Riveros, *Chem. Phys. Lett.*, **355** (2002) 543.
[129] C. Curutchet, A. Bidon-Chanal, I. Soteras, M. Orozco and F. J. Luque, *J. Phys. Chem. B*, **109** (2005) 3565.
[130] G. I. Almerindo, D. W. Tondo and J. R. Pliego Jr., *J. Phys. Chem. A*, **108** (2004) 166.
[131] Y. Fu, L. Liu, R. Li, R. Liu and Q. Guo, *J. Am. Chem. Soc.*, **126** (2004) 814.
[132] J. R. Pliego, Jr. and J. M. Riveros, *J. Phys. Chem. A*, **106** (2002) 7434.
[133] S. Miertius, E. Scrocco and J. Tomasi, *Chem. Phys.*, **55** (1981) 117.
[134] R. Cammi and J. Tomasi, *J. Comput. Chem.*, **16** (1995) 1449.
[135] V. Barone, M. Cossi and J. Tomasi, *J. Chem. Phys.*, **107** (1997) 3210.
[136] A. Klamt and G. Schüürmann, *J. Chem. Soc. Perkin Trans.* **2** (1993) 799.
[137] F. Eckert and A. Klamt, *Am. Inst. Chem. Eng. J.*, **48** (2002) 369.
[138] A. Klamt, V. Jonas, T. Bürger and J. C. W. Lohrenz, *J. Phys. Chem. A*, **102** (1998) 5074.
[139] T. N. Truong, U. N. Nguyen and E. V. Stefanovich, *Int. J. Quantum Chem.*, **1996** (1996) 1615.
[140] V. Baroni and M. Cossi, *J. Phys. Chem. A*, **102** (1998) 1995.
[141] C. Gonzalez, A. Restrepo-Cossio, M. Márquez, K. B. Wiberg and M. DeRosa, *J. Phys. Chem. A*, **102** (1998) 2732.
[142] T. N. Truong and E. V. Stefanovich, *J. Phys. Chem.*, **99** (1995) 14700.
[143] A. A. Mohamed and F. Jensen, *J. Phys. Chem. A*, **105** (2001) 3259.
[144] B. L. Kormos and C. J. Cramer, *J. Org. Chem.*, **68** (2003) 6375.
[145] G. Vayner, K. N. Houk, W. L. Jorgensen and J. I. Brauman, *J. Am. Chem. Soc.*, **126** (2004) 9054.
[146] S. J. Mo, T. Vreven, B. Mennucci, K. Morokuma and J. Tomasi, *Theor. Chem. Acc.*, **111** (2004) 154.
[147] D. W. Tondo and J. R. Pliego Jr., *J. Phys. Chem. A*, **109** (2005) 507.
[148] J. R. Pliego Jr., *J. Mol. Catal. A*, **239** (2005) 228.
[149] G. I. Almerindo and J. R. Pliego Jr., *Org. Lett.*, **7** (2005) 1821.
[150] G. I. Almerindo and J. R. Pliego Jr., *Chem. Phys. Lett.*, **423** (2006) 459.
[151] Y. Fang, Y. Gao, P. Ryberg, J. Eriksson, M. Kolodziejska-Huben, A. Dybala-Defratyka, S. Madhavan, R. Danielsson, P. Paneth, O. Matsson and K. C. Westaway, *Chem. Eur. J.*, **9** (2003) 2696.
[152] J. R. Pliego Jr. and J. M. Riveros, *J. Phys. Chem. A*, **108** (2004) 2520.
[153] S. Antonczak, M. F. Ruiz-Lopez and J. L. Rivail, *J. Am. Chem. Soc.*, **116** (1994) 3912.
[154] D. Sicinska, D. G. Truhlar and P. Paneth, *J. Am. Chem. Soc.*, **123** (2001) 7683.
[155] X. Assfeld, J. Garapon, D. Rinaldi, M. F. Ruiz-Lopez and J. L. Rivail, *Theochem*, **371** (1996) 107.
[156] A. Gonzàlez-Lafont and D. G. Truhlar, in E. R. Bernstein (eds), *Chemical Reactions in Clusters*, Oxford University Press, New York, 1996, pp 1–39.
[157] D. Sicinska, P. Paneth and D. G. Truhlar, *J. Phys. Chem. B*, **106** (2002) 2708.
[158] J. R. Pliego Jr. and J. M. Riveros, *Chem. Eur. J.*, **8** (2002) 1945.

[159] J. R. Pliego Jr., *Chem. Phys.*, **306** (2004) 273.
[160] J. F. Marlier, *J. Am. Chem. Soc.*, **115** (1993) 5935.
[161] J. Blumberger and M. L. Klein, *Chem. Phys. Lett.*, **422** (2006) 210.
[162] J. Blumberger, B. Ensing and M. L. Klein, *Angew. Chem. Int. Ed.*, **45** (2006) 2893.
[163] D. A. Liotard, G. D. Hawkins, G. C. Lynch, C. J. Cramer and D. G. Truhlar, *J. Comput. Chem.*, **16** (1995) 422.
[164] M. Solà, A. Lledós, M. Duran, J. Bertrán and J.-L. M. Abboud, *J. Am. Chem. Soc.*, **113** (1991) 3873.
[165] T. N. Truong, T. T. T. Truong and E. V. Stefanovich, *J. Chem. Phys.*, **107** (1997) 1881.
[166] H. Castejon and K. B. Wiberg, *J. Am. Chem. Soc.*, **121** (1999) 2139.
[167] K. Ohmiya and S. Kato, *J. Chem. Phys.*, **119** (2003) 1601.
[168] M. F. Ruasse, *Adv. Phys. Org. Chem.*, **28** (1993) 207.
[169] M. Cossi, M. Persico and J. Tomasi, *J. Am. Chem. Soc.*, **116** (1994) 5373.
[170] X. Assfeld, J. Garapon, D. Rinaldi, M. F. Ruiz-Lopez and J. L. Rivail, *Theochem*, **371** (1996) 107.
[171] T. Koerner, R. S. Brown, J. L. Gainsforth and M. Klobukowski, *J. Am. Chem. Soc.*, **120** (1998) 5628.
[172] Y. Kurosaki, *Theochem*, **503** (2000) 231.
[173] Y. Kurosaki, *Theochem*, **545** (2001) 225.
[174] Y. Kurosaki, *J. Phys. Chem. A*, **105** (2001) 11080.
[175] L. Gorb, A. Asensio, I. Tuñón and M. F. Ruiz-López, *Chem. Eur. J.*, **11** (2005) 6743.
[176] R. Cammi, B. Mennucci, C. Pomelli, C. Capelli, S. Corni, L. Frediani, G. W. Trucks and M. J. Frisch, *Theor. Chem. Acc.*, **111** (2004) 66.
[177] M. L. Poutsma and J. L. Kartch, *Tetrahedron*, **22** (1966) 2167.
[178] S. M. Resende, J. R. Pliego Jr. and W. B. de Almeida, *J. Chem. Soc. Faraday Trans.*, **94** (1998) 2895.
[179] D. Xie, D. Xu, L. Zhang and H. Guo, *J. Phys. Chem. B*, **109** (2005) 5259.
[180] J. P. Guthrie, *J. Am. Chem. Soc.*, **113** (1991) 3941.
[181] T. H. Rod, P. Rydberg and U. Ryde, *J. Chem. Phys.*, **124** (2006) 174503.
[182] J. Gao and D. G. Truhlar, *Annu. Rev. Phys. Chem.*, **53** (2002) 467.
[183] H. Nymeyer and A. E. Garcia, *Proc. Natl Acad. Sci. USA*, **100** (2003) 13934.
[184] C. M. Stultz, *J. Phys. Chem. B*, **108** (2004) 16525.
[185] R. Zhao, *Proteins*, **53** (2003) 148.
[186] J. W. Storer, D. J. Giesen, G. D. Hawkins, G. C. Lynch, C. J. Cramer, D. G. Truhlar and D. A. Liotard, in C. J. Cramer and D. G. Truhlar (eds), *Structure and Reactivity in Aqueous Solution*, American Chemical Society, Washington, DC, 1994, pp 24–49.
[187] D. L. Severance and W. L. Jorgensen, *J. Am. Chem. Soc.*, **114** (1992) 10966.
[188] W. L. Jorgensen, J. F. Blake, D. Lim and D. L. Severance, *J. Chem. Soc. Faraday, Trans.*, **90** (1994) 1727.
[189] J. Gao, *J. Am. Chem. Soc.*, **116** (1994) 1563.
[190] C. J. Cramer and D. G. Truhlar, *J. Am. Chem. Soc.*, **114** (1993) 8794.
[191] A. Delabie, S. Creve, B. Coussens and M. T. Nguyen, *J. Chem. Soc. Perkin Trans.*, **2** (2000) 977.
[192] P. Ulanski, G. Merenyi, J. Lind, R. Wagner and C. V. Sonntag, *J. Chem. Soc. Perkin*, **2** (1999) 673.
[193] Y.-Y. Chuang, M. Radhakrishnan, P. L. Fast, C. J. Cramer and D. G. Truhlar, *J. Phys. Chem. A*, **103** (1999) 4893.
[194] A. Lossack, E. Roduner and D. M. Bartels, *J. Phys. Chem. A*, **102** (1998) 7462.
[195] M. Anbar and D. Meyerstein, *J. Phys. Chem.*, **68** (1964) 3184.
[196] J. Pu and D. G. Truhlar, *J. Phys. Chem. A*, **109** (2005) 773.

[197] G. Tresadern, J. Willis, I. Hillier and C. I. F. Watt, *Phys. Chem. Chem. Phys.*, **3** (2001) 3967.
[198] G. Raspert, M. T. Nguyen, S. Kelly and A. F. Hegarty, *J. Org. Chem.*, **63** (1998) 9669.
[199] A. Cavalli, M. Masetti, M. Recantini, C. Prandi, A. Guarna and E. G. Occhiato, *Chem. Eur. J.*, **12** (2006) 2836.
[200] G. A. DiLabio and K. U. Ingold, *J. Org. Chem.*, **69** (2004) 1620.
[201] H. C. Brown and Y. Okamoto, *J. Am. Chem. Soc.*, **80** (1958) 4979.
[202] N. Kornblum, H. O. Larson, R. K. Blackwood, D. D. Mooberry, E. P. Oliveto and G. E. Graham, *J. Am. Chem. Soc.*, **78** (1956) 1497.
[203] E. Westphal and J. R. Pliego Jr., *J. Phys. Chem. A*, **111** (2007) in press.
[204] P. K. Das, D. W. Dockter, D. R. Fahey, D. E. Lauffer, G. D. Hawkins, J. Li, T. Zhu, C. J. Cramer, D. G. Truhlar, S. Dapprich, R. D. J. Froese, M. C. Holthausen, Z. Liu, K. Mogi, S. Viboishchikov, D. G. Musaev and K. Morokuma, in D. G. Truhlar and K. Morokuma (eds), *Transition State Modeling for Catalysis*, ACS Symp. Ser. 721, American Chemical Society, Washington, DC, 1999, pp 208–224.
[205] M. Graf, K. Angermund, G. Fink, W. Thiel and V. R. Jensen, *J. Organomet. Chem.*, **691** (2006) 4367.
[206] R. J. Nielsen and W. A. Goddard, III, *J. Am. Chem. Soc.*, **128** (2006) 9651.
[207] J. R. Pliego Jr., *Org. Biomol. Chem.*, **4** (2006) 1667.
[208] O. N. Ventura, A. Lledos, R. Bonaccorsi, J. Bertran and J. Tomasi, *Theor. Chim. Acta*, **72** (1987) 175.
[209] D. Lim, C. Jensen, M. P. Repasky and W. L. Jorgensen, in D. G. Truhlar and K. Morokuma (eds) *Transition State Modeling for Catalysis*, ACS Symp. Ser. 721, American Chemical Society, Washington, DC, 1999, pp 74–85.
[210] L. Rodriguez-Santiago, O. Vendrell, I. Tejero, M. Sodupe and J. Bertran, *Chem. Phys. Lett.*, **334** (2001) 112.